Coherent imaging methods with XFELs

Rick Kirian
Arizona State University

FEISII

May 9, 2015

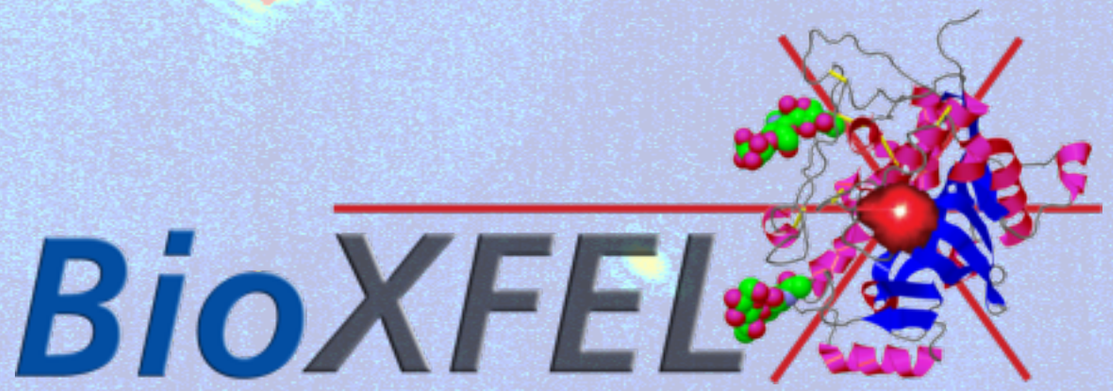

Imaging biomolecules through XFEL “serial diffraction”

Nanocrystal diffraction
Solution-phase diffraction
Gas-phase, single-particle diffraction

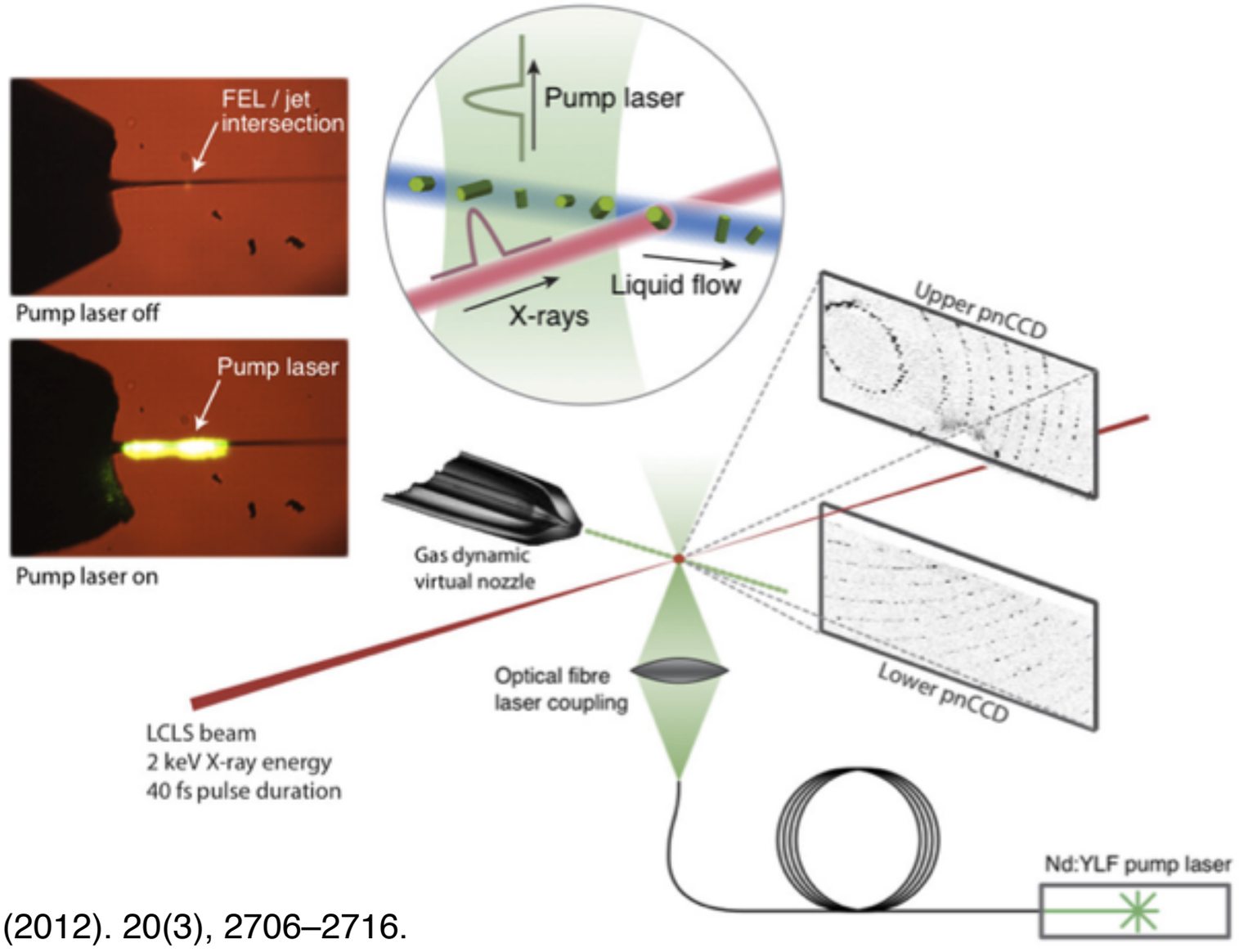

Aquila, A.,, et al. (2012). 20(3), 2706–2716.

XFELs produce intensities away from the Bragg condition

$$I(\mathbf{q}) \propto |F(\mathbf{q})|^2 |S(\mathbf{q})|^2$$

Diffraction intensity = | unit cell transform |^2 x | lattice transform |^2

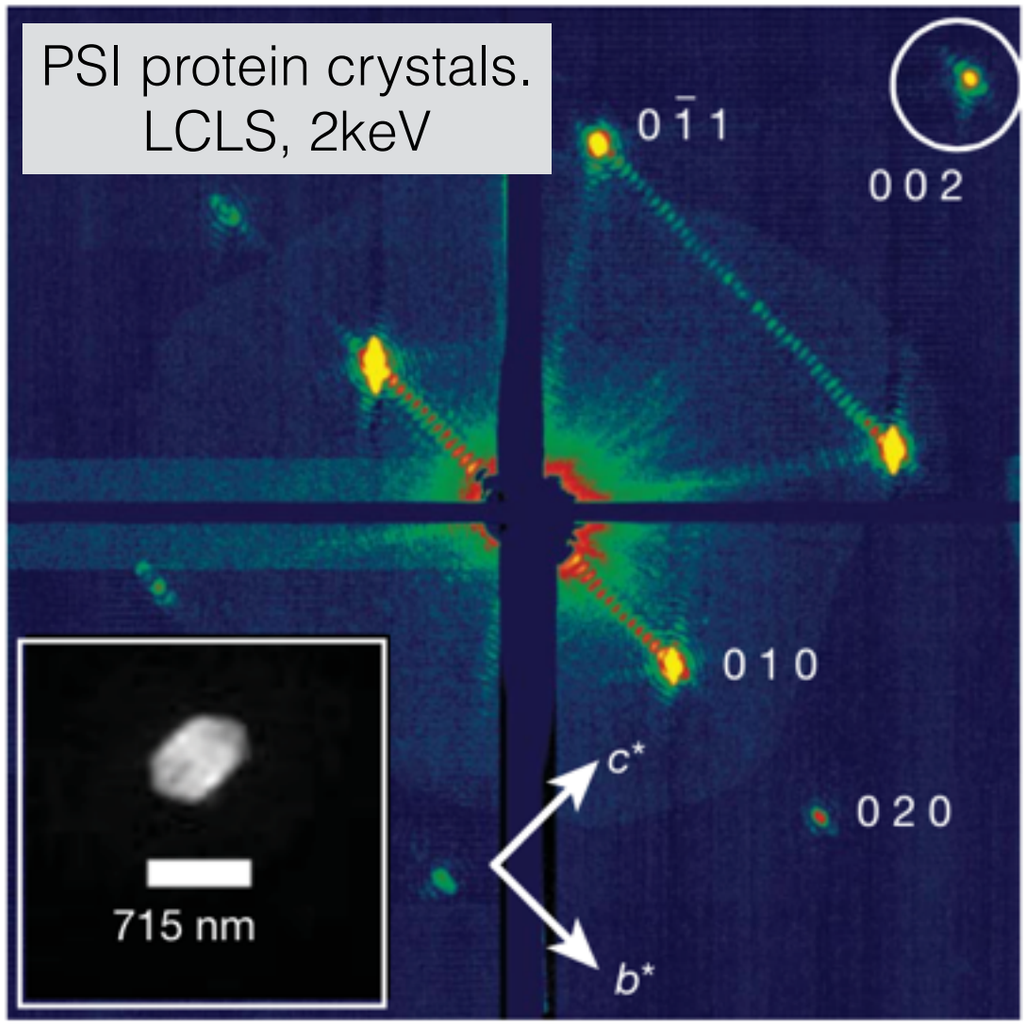

Chapman, H. N., et al. (2011). *Nature*, *470*(7332), 73–U81.

Gold crystals, laser pumped

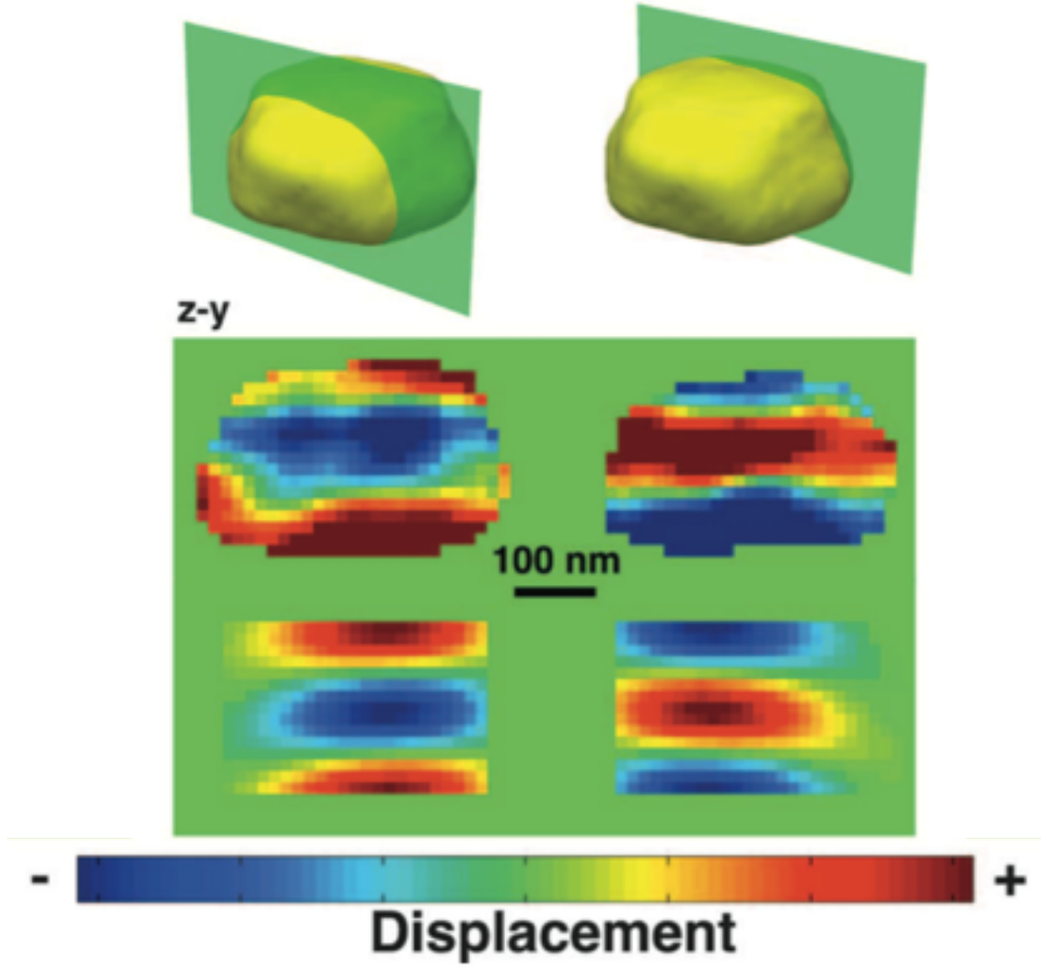

Clark, J. N.,, et al. (2013). Science, 341(6141), 56–59.

“Over-sampling” solves the crystallographic phase problem!

$$I(\mathbf{q}) \propto |F(\mathbf{q})|^2 |S(\mathbf{q})|^2$$

Diffraction intensity = | unit cell transform |^2 x | lattice transform |^2

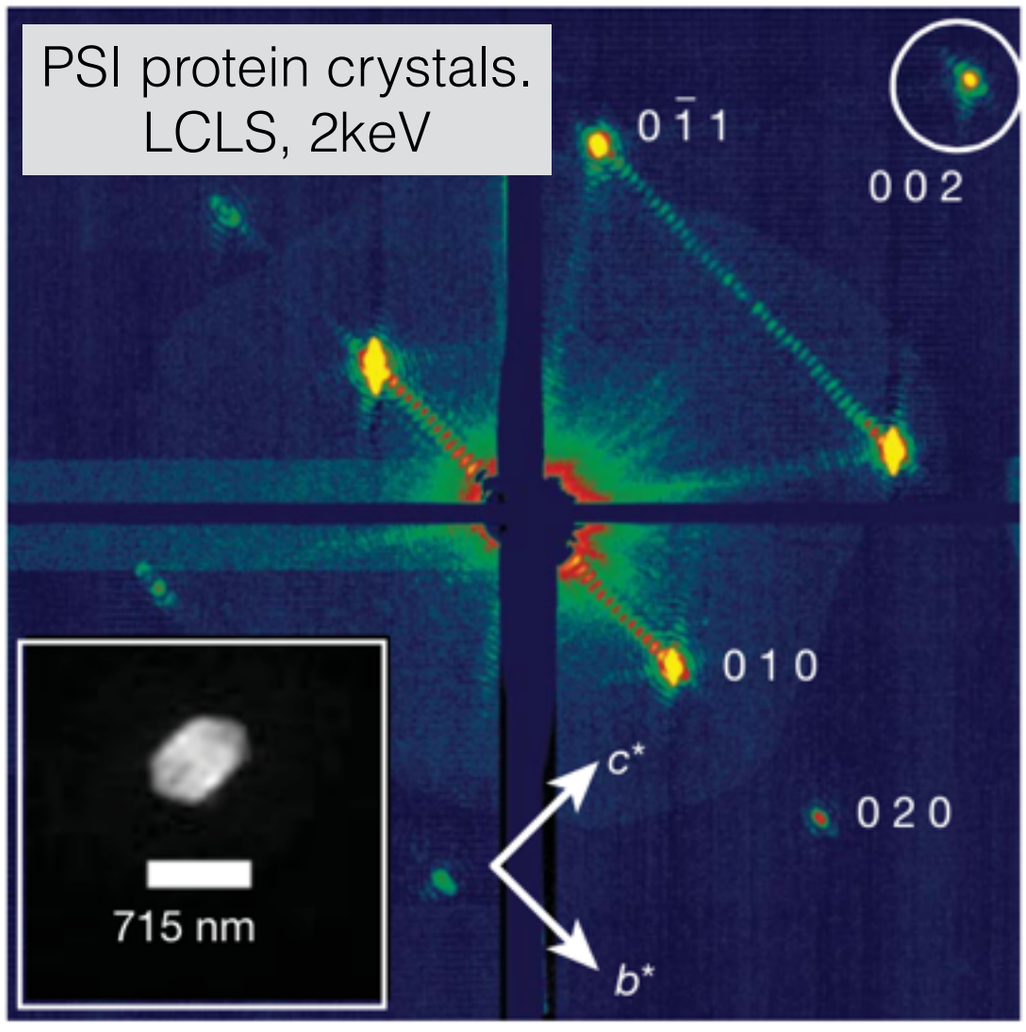

Chapman, H. N., et al. (2011). *Nature*, *470*(7332), 73–U81.

Sampling between the Bragg peaks completely determines an un-aliased autocorrelation function of the unit cell.

An un-aliased autocorrelation solves the crystallographic phase problem without…

- *Prior-known structure information*
- *Resonant conditions*
- *Sample modification*
- *Resolution restrictions*

How can we exploit the lattice-transformed intensities?

$$I(\mathbf{q}) \propto |F(\mathbf{q})|^2 \langle |S(\mathbf{q})|^2 \rangle$$

average diffraction intensity = | unit cell transform |^2 x avg(| lattice transform |^2)

How can we exploit the lattice-transformed intensities?

$$I(\mathbf{q}) \propto |F(\mathbf{q})|^2 \langle |S(\mathbf{q})|^2 \rangle$$

average diffraction intensity = | unit cell transform |^2 x avg(| lattice transform |^2)

$$|F(\mathbf{q})|^2 \propto I(\mathbf{q}) / |S(\mathbf{q})|^2$$

| unit cell transform |^2 = average diffraction intensity / avg(| lattice transform |^2)

Spence, J. C. H., Kirian, R. A., et al. (2011). *Optics Express*, *19*(4), 2866.

Demonstration of phasing simple crystal data, soft-x-ray FEL

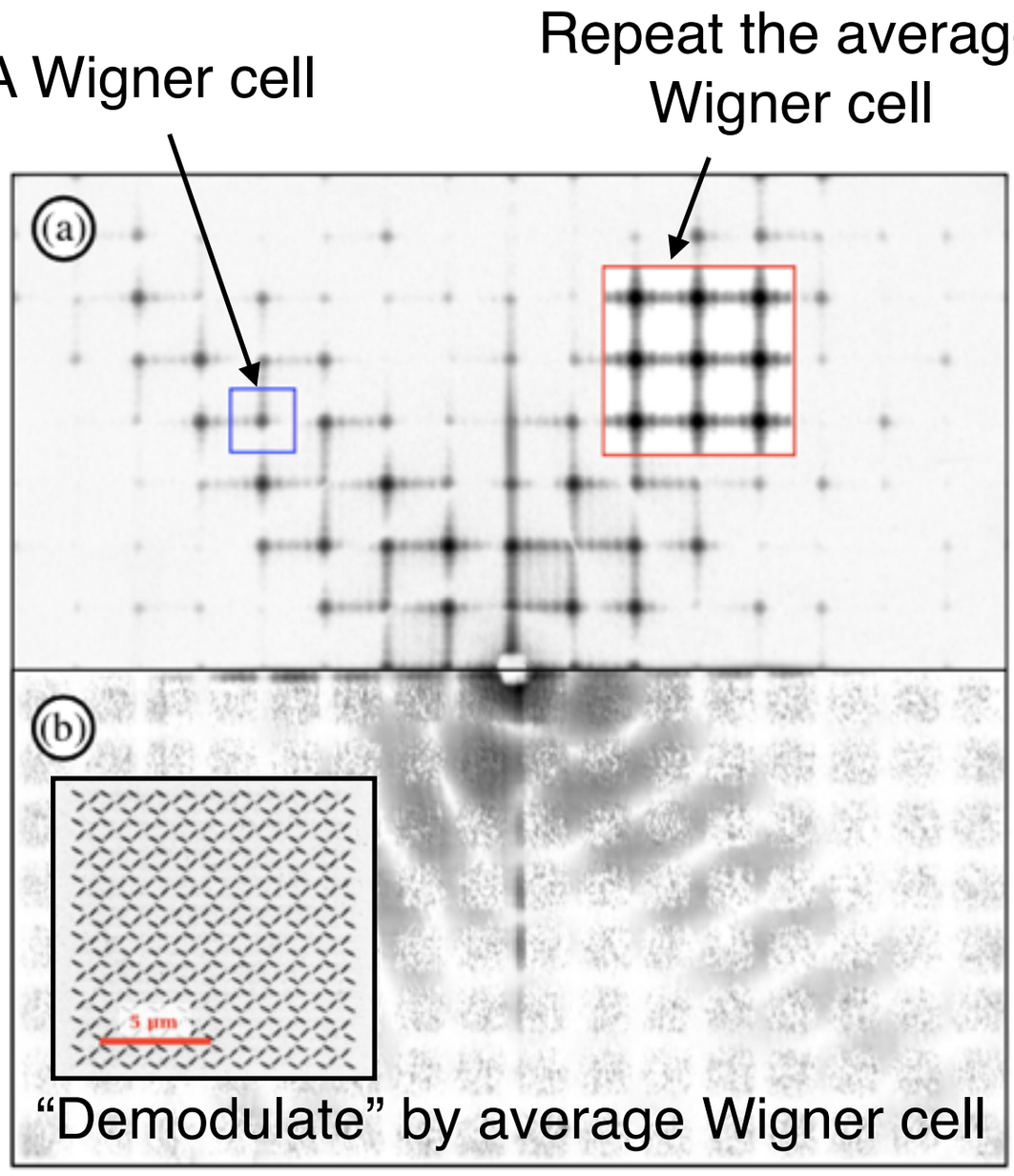

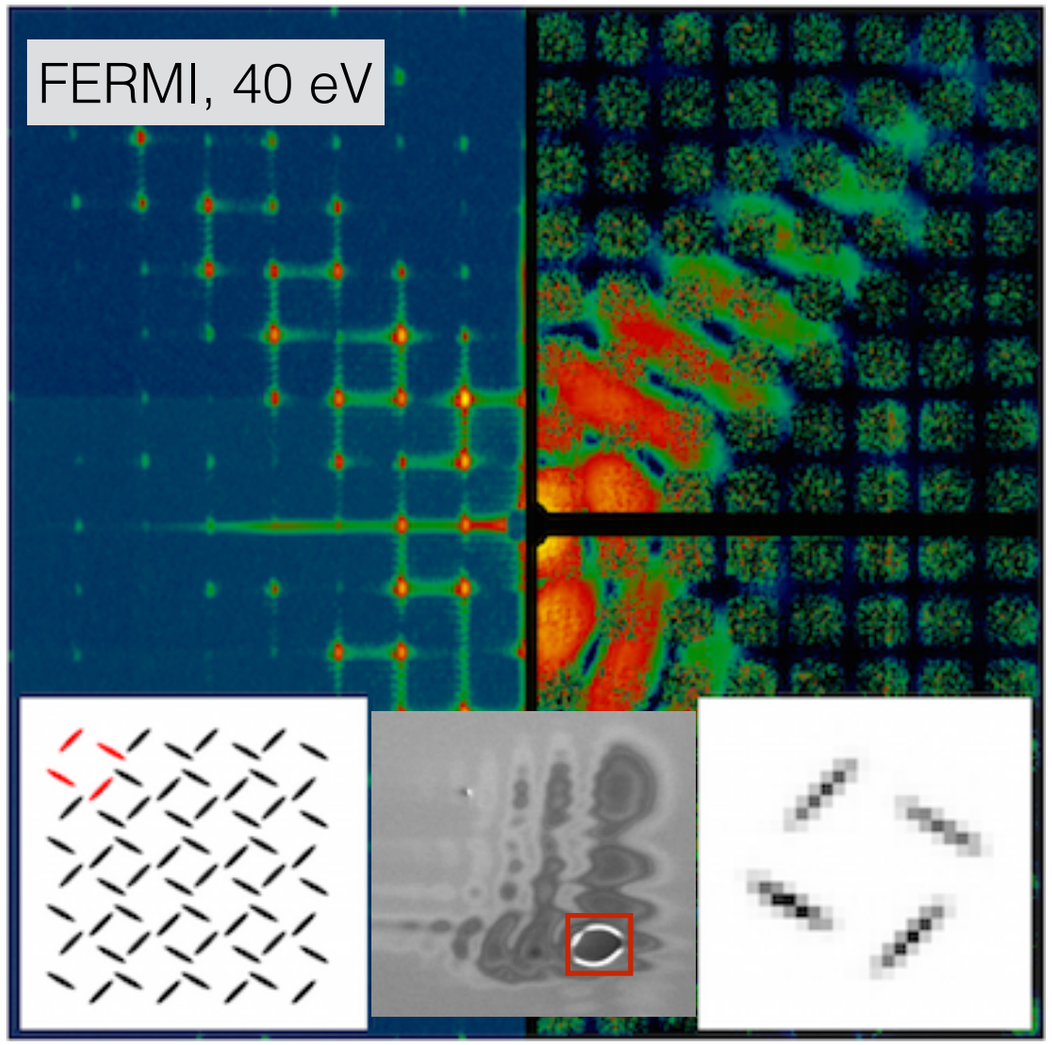

Experimental measurements at the FERMI soft-x-ray FEL

Kirian, R. A., et al. (2015). Physical Review X, 5(1), 011015–12.

What is the “unit cell” of a finite crystal?

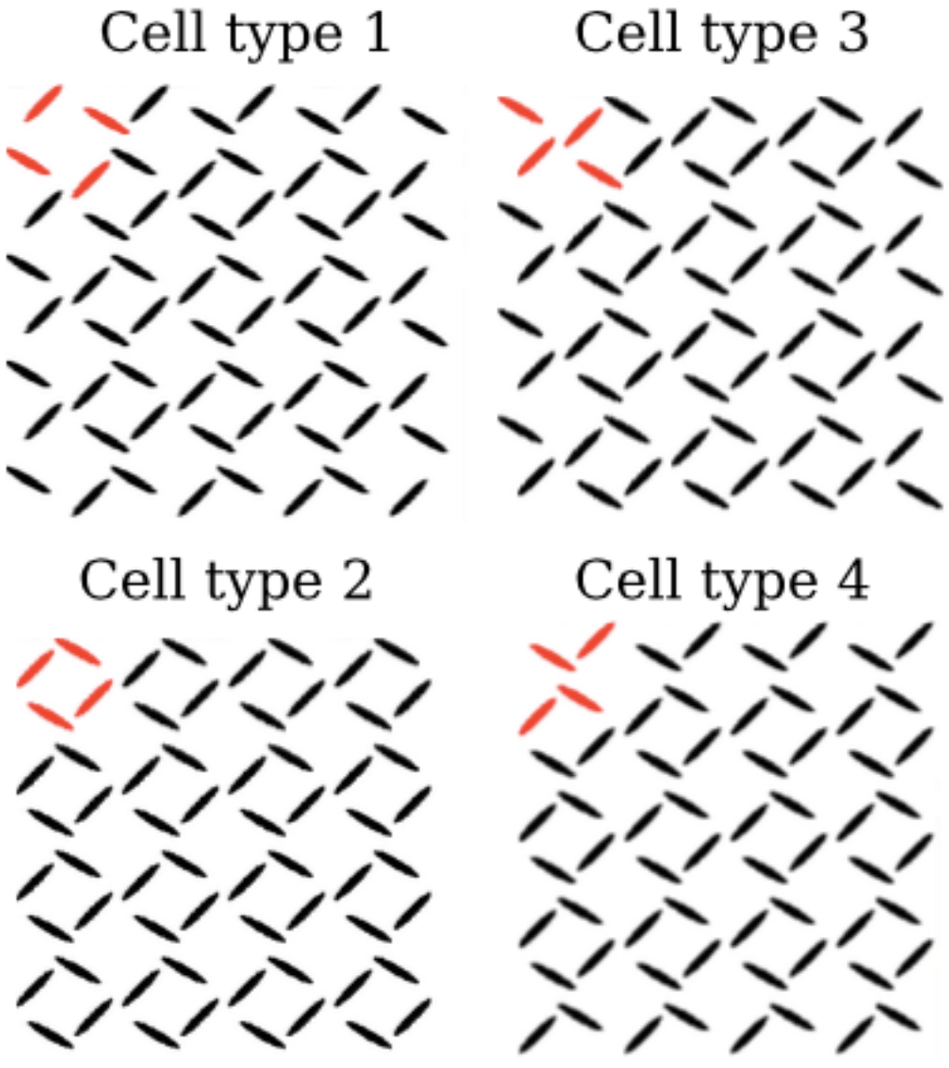

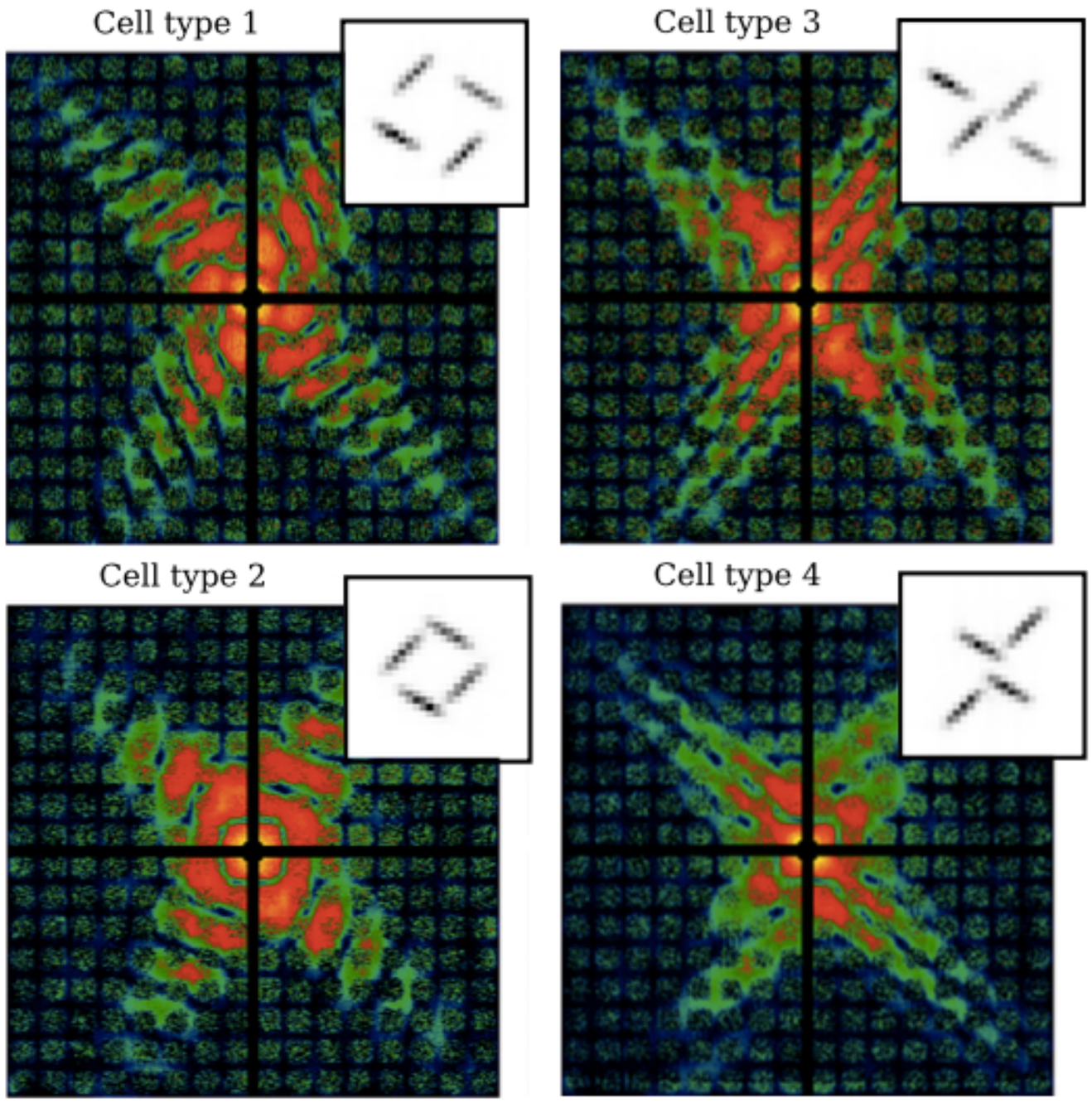

Kirian, R. A., et al. (2015). Physical Review X, 5(1), 011015–12.

Some crystals have no “unit cell”!

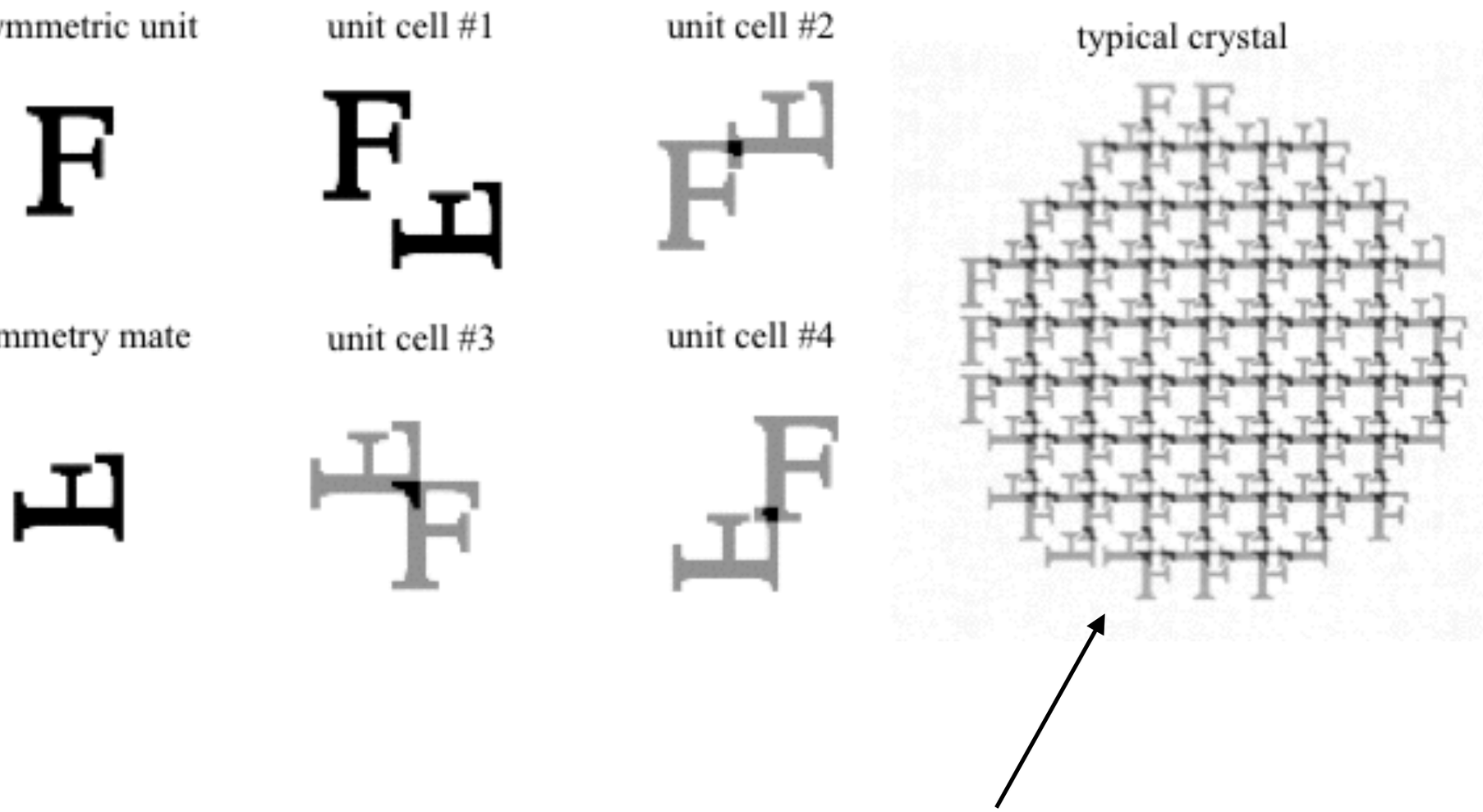

This crystal has no unique unit cell! Instead, it has contributions from many unit cells.

Kirian, R. A., *et al.* (2014). Phil. Trans. B. 369(1647), 20130331–20130331.

Some crystals have no “unit cell”!

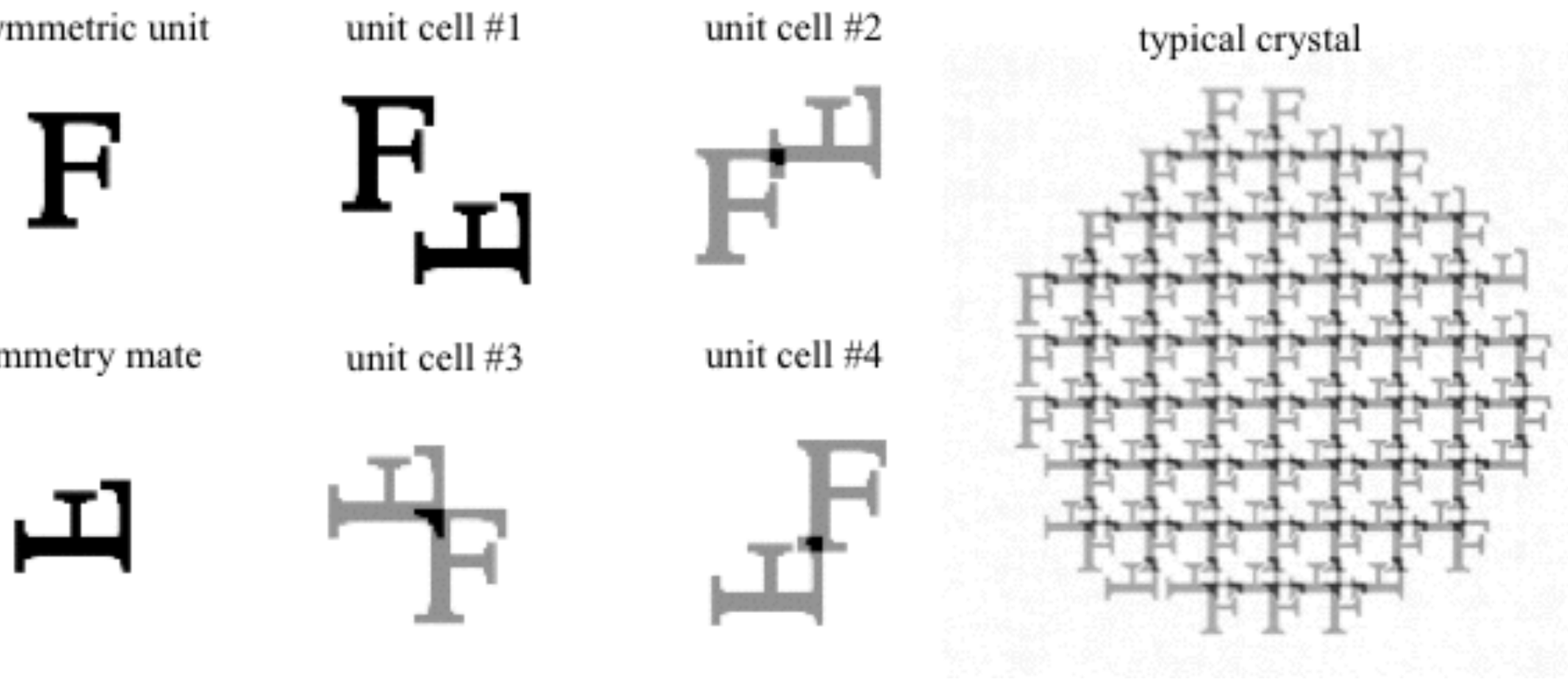

$$I(\mathbf{q}) \propto |F(\mathbf{q})|^2 \langle |S(\mathbf{q})|^2 \rangle$$

Kirian, R. A., *et al.* (2014). Phil. Trans. B. 369(1647), 20130331–20130331.

Some crystals have no “unit cell”!

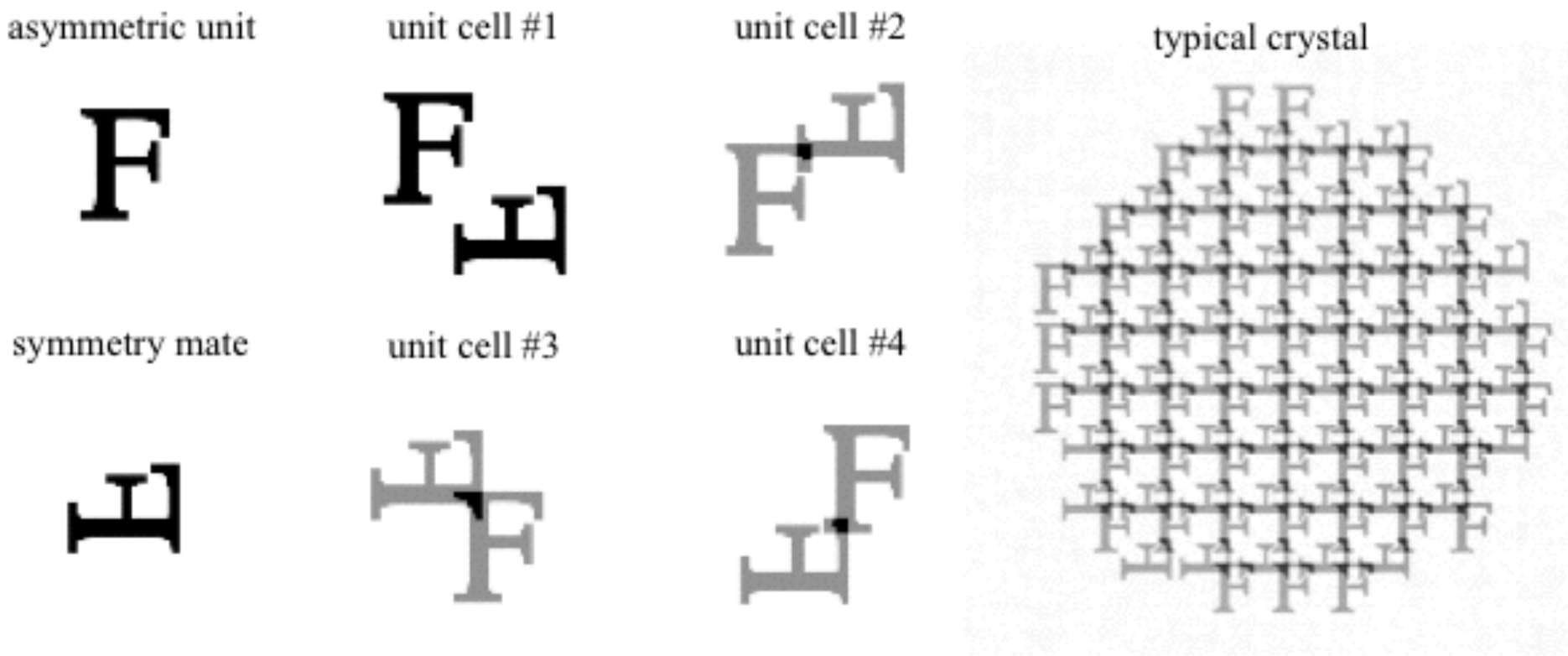

Fix the projection operator in the phasing algorithm
(a “modal decomposition” of the intensities)

$$\widetilde{P}_{\mathrm{I}}\,\tilde{\rho}_i(\boldsymbol{q}) = \tilde{\rho}_i(\boldsymbol{q})\sqrt{\frac{I(\boldsymbol{q})}{\frac{1}{4}\sum_{n=1}^{4}\left|\tilde{\rho}_i(\boldsymbol{q}) + \tilde{\rho}_i(\mathbf{R}^{\mathrm{T}}\boldsymbol{q})\mathrm{e}^{-\mathrm{i}\boldsymbol{q}\cdot\mathrm{t}_n}\right|^2}}.$$

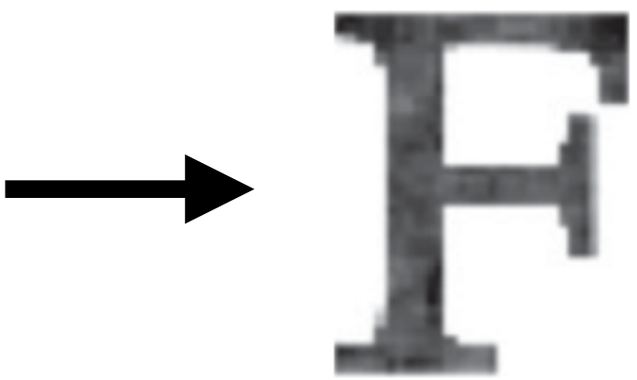

Kirian, R. A., *et al.* (2014). Phil. Trans. B. 369(1647), 20130331–20130331.

Continuum diffraction field in serial protein crystallography

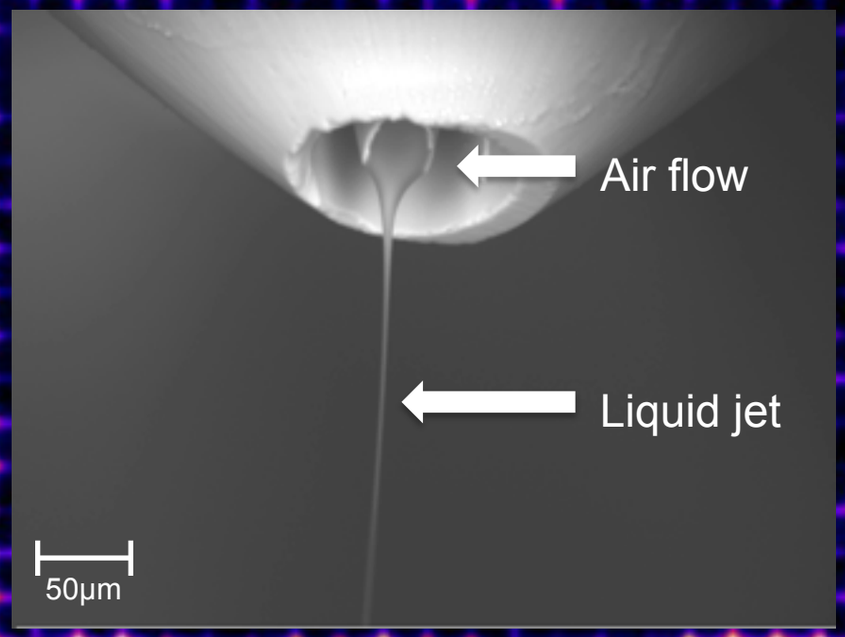

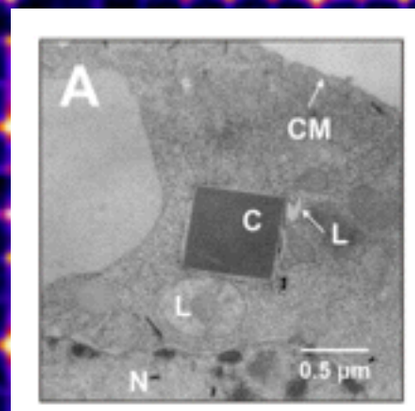

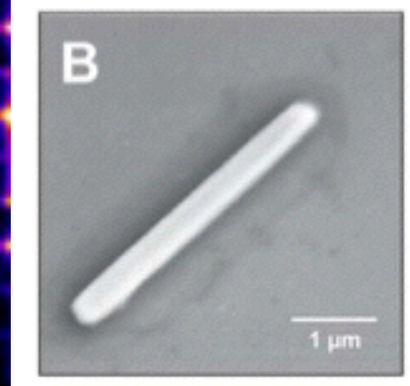

Yefanov, O., et al. (2014). *Phil. Trans. B*, *369*(1647), 20130333–20130333.

Serial femtosecond crystallography is a powerful technique!

1) Overcome radiation damage
2) Smaller (and more perfect?) crystals, higher throughput
3) Room-temperature studies
4) Time resolution, and irreversible processes
5) A general de-novo solution to the phase problem?

… but what if we just don’t have crystals?

~~Nanocrystal diffraction~~

Solution-phase diffraction

Gas-phase, single-particle diffraction

Z. Kam's remarkable angular correlation idea

randomly-oriented
molecules frozen in
space or time

Snapshot diffraction
pattern, with angular fluctuations

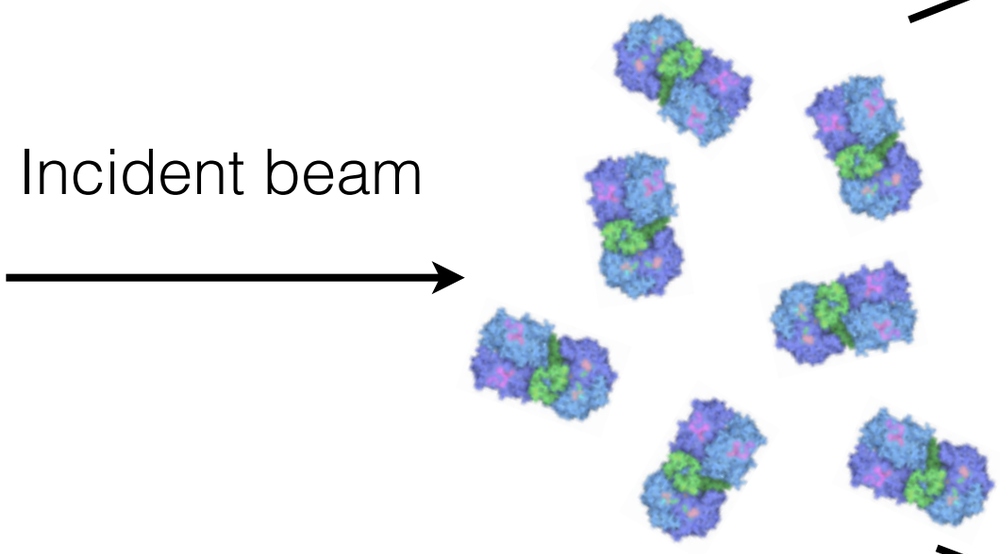

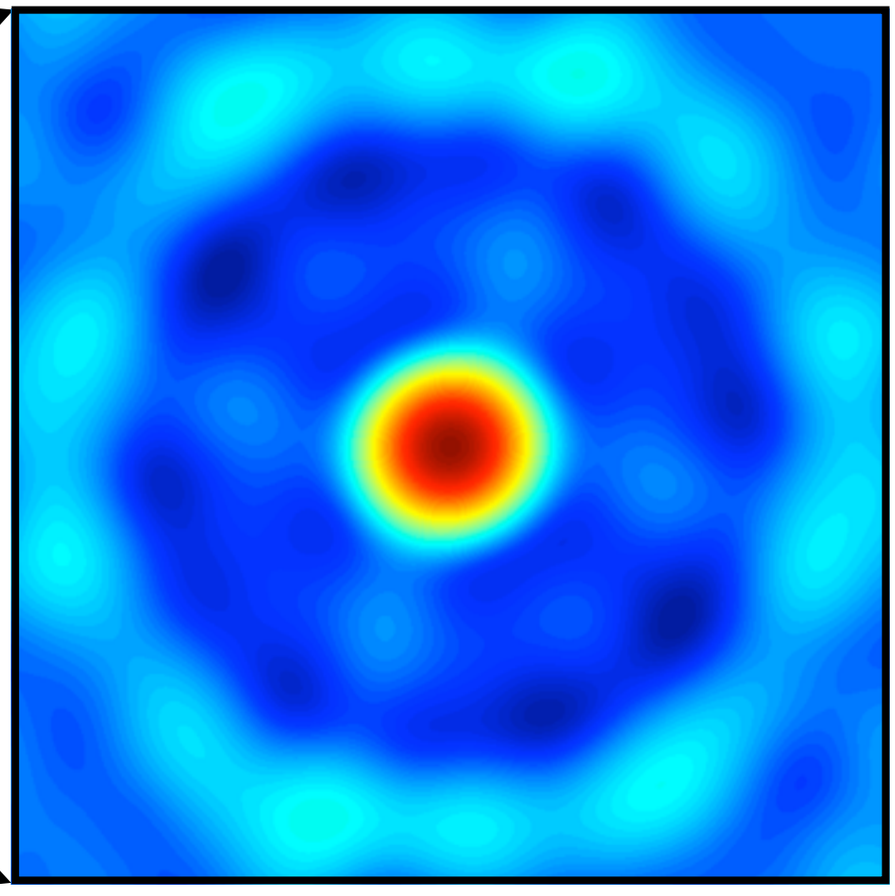

Incident beam

X-ray pulse must be shorter
than rotational diffusion time

Kam, Z. (1977). Macromolecules, 10(5), 927–934.

Z. Kam's remarkable angular correlation idea

Kam's measurement:

Ring 1 intensity: $I(q, \phi)$

Ring 2 intensity: $I(q', \phi')$

Angular cross correlation:

$$C(q, q', \Delta\phi) = \frac{1}{2\pi} \int_0^{2\pi} I(q, \phi) I(q', \phi - \Delta\phi) d\phi$$

Snapshot diffraction pattern, with angular fluctuations

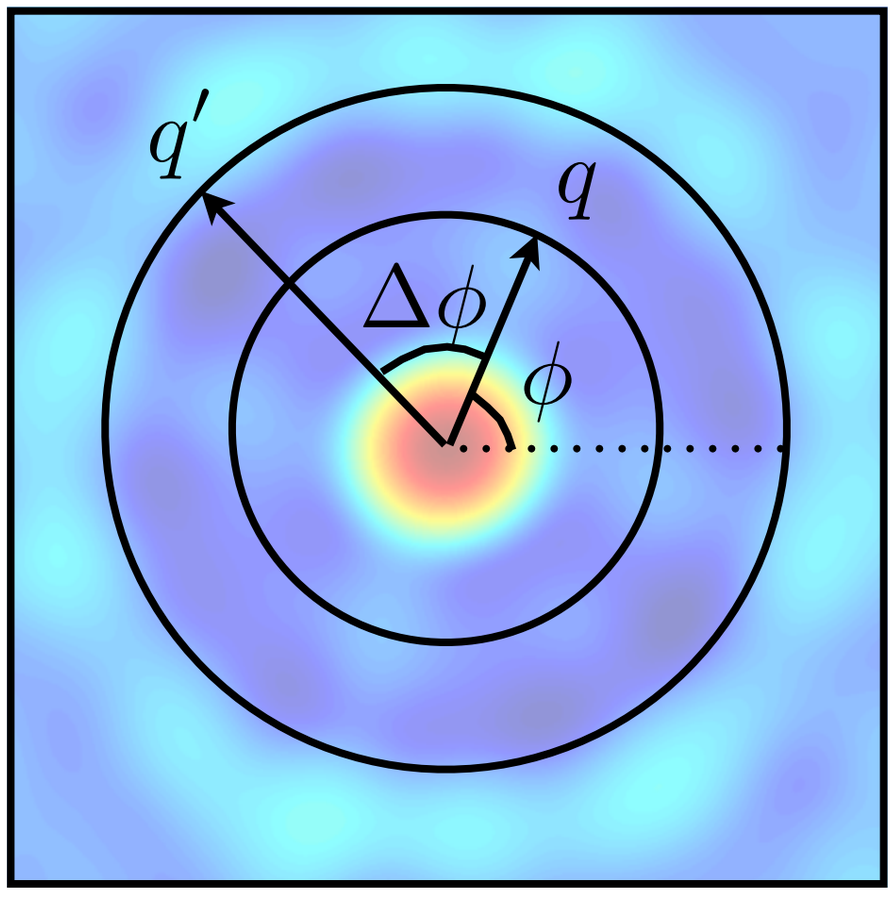

Kam, Z. (1977). Macromolecules, 10(5), 927–934.

Z. Kam's remarkable angular correlation idea

Kam's measurement:

Ring 1 intensity: $I(q, \phi)$

Ring 2 intensity: $I(q', \phi')$

Angular cross correlation:

$$C(q, q', \Delta\phi) = \frac{1}{2\pi} \int_0^{2\pi} I(q, \phi) I(q', \phi - \Delta\phi) d\phi$$

This reduces to the correlation of just one molecule!

Snapshot diffraction pattern, with angular fluctuations

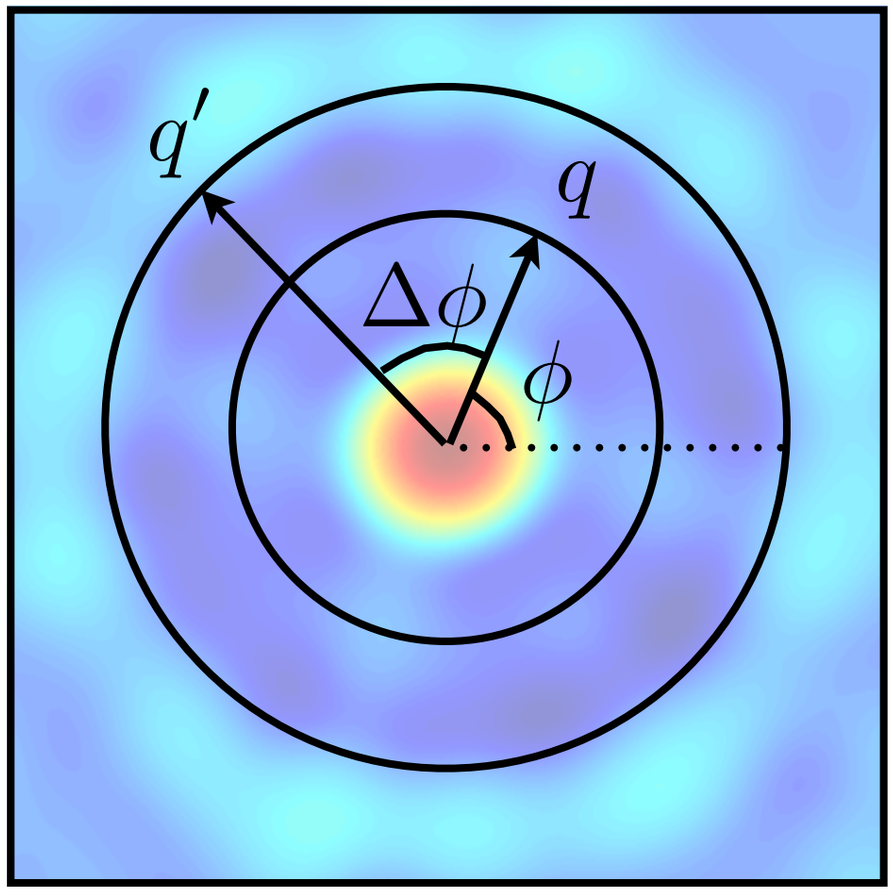

Kam, Z. (1977). Macromolecules, 10(5), 927–934.

Imaging with angular correlations

The problem of forming images from ensembles of particles aligned about an axis has been solved, many times over

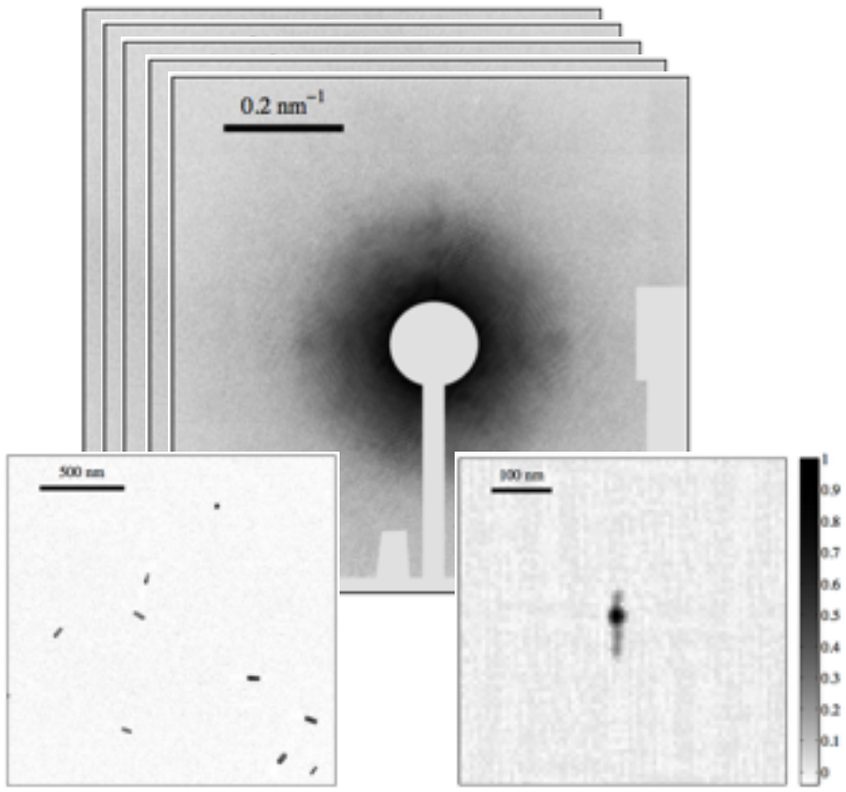

Pair correlations, x-ray diffraction:
Saldin, D. K., et al. (2011). *Phys. Rev. Lett.*, *106*(11), 115501.

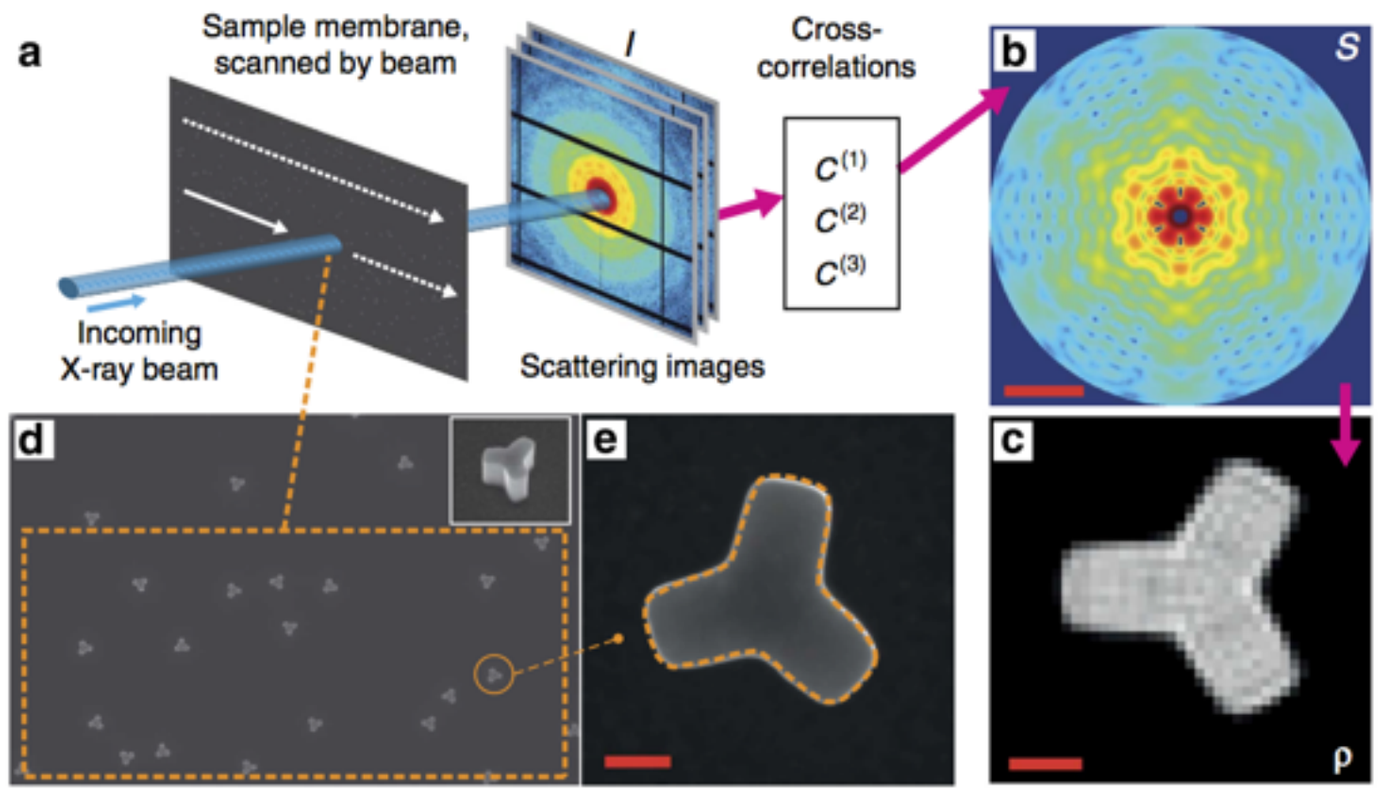

Triple correlations, x-ray diffraction
Pedrini, B., et al. (2013). *Nature Comm.*, *4*, 1647.

2D stained electron micrographs
Kam, Z., Gafni, I., & Kessel, M. (1982). *Ultramicroscopy*, *7*(4), 311–320.

Non-iterative solution, triple correlation simulations
Kurta, R. P., *et al.* (2013). *New Journal of Physics*, *15*(1), 013059

3D methods continue to evolve

"SAXS-plus" model building (minimize model-measurement errors)

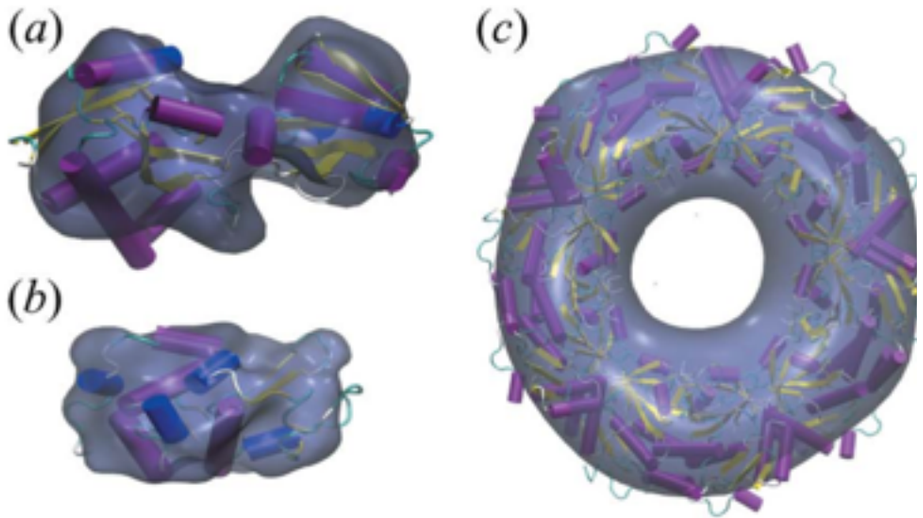

Liu, H., *et al.* Acta Cryst. A 69, (2013).

Symmetry constraints along with iterative phasing

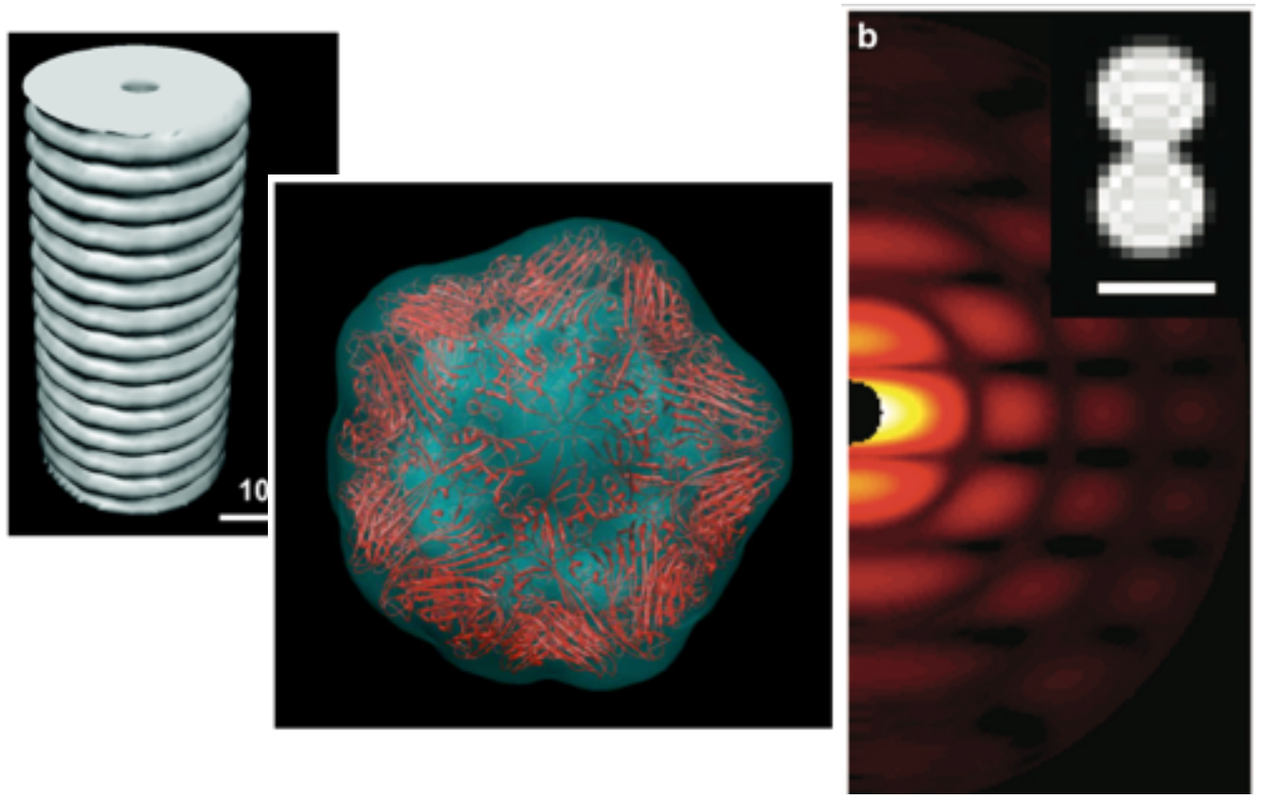

Saldin, D., *et al.* Optics Express 19, 17318–17335 (2011).

Poon, H. C., *et al.* Physical Review Letters 110, 265505 (2013).

Starodub, D., *et al*. Nature Communications, *3*, 1276–7 (2012).

A 3D difference map can be determined directly!

Assume ground state structure is known

Use variation method on reduced data

$$\delta B_l(q, q') = \sum_m \delta I_{lm}(q) I^*_{lm}(q') + I_{lm}(q) \delta I^*_{lm}(q')$$

A *non-iterative* approach exists for solving this problem, directly revealing a real-space difference map!!

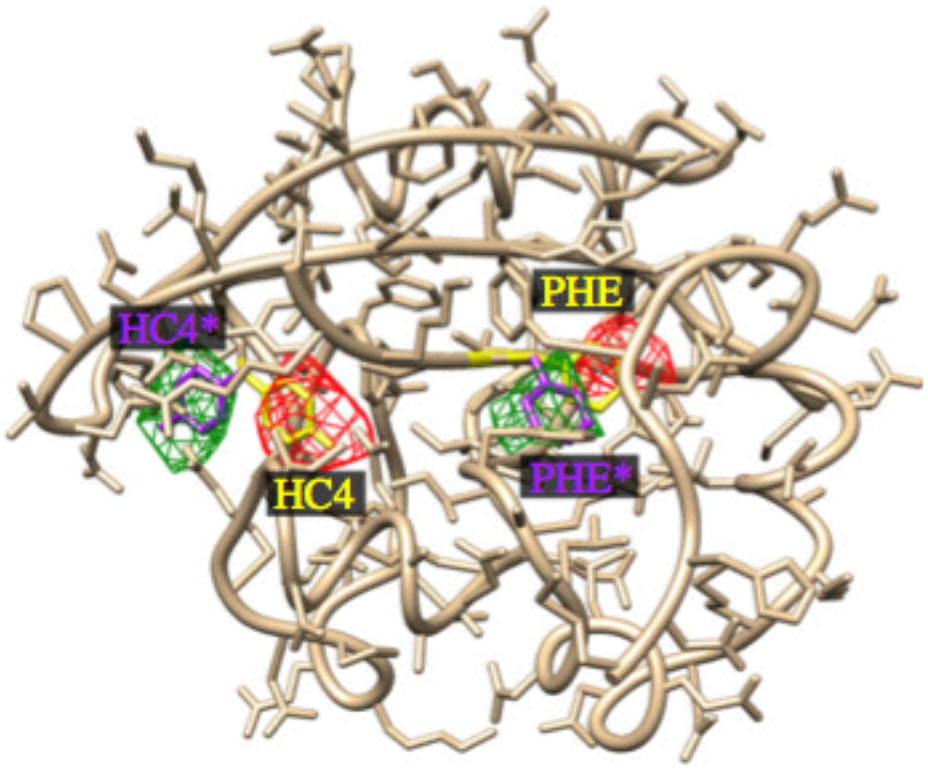

Difference map solved from simulated intensities (noise-free) from PYP protein molecules.

Pande, K., *et al*. Phil. Trans. B: Biological Sciences 369 (2014).

We have considered signal and noise in detail…

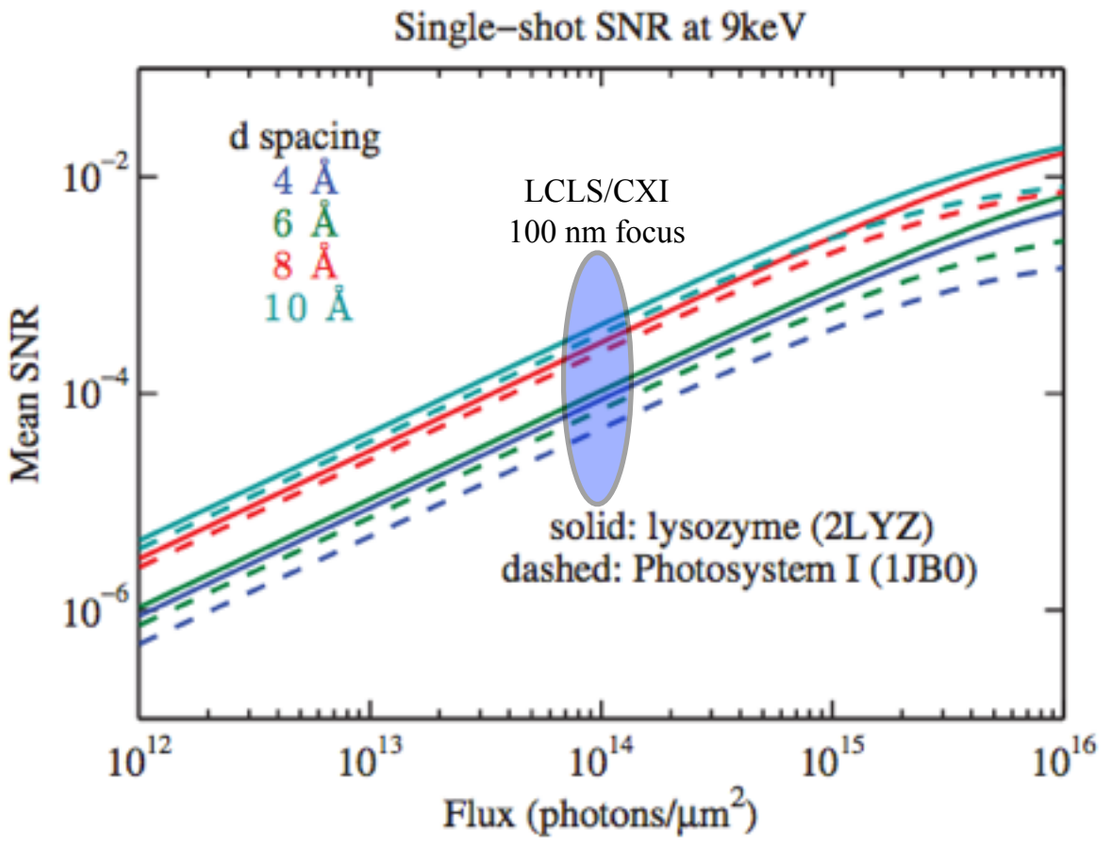

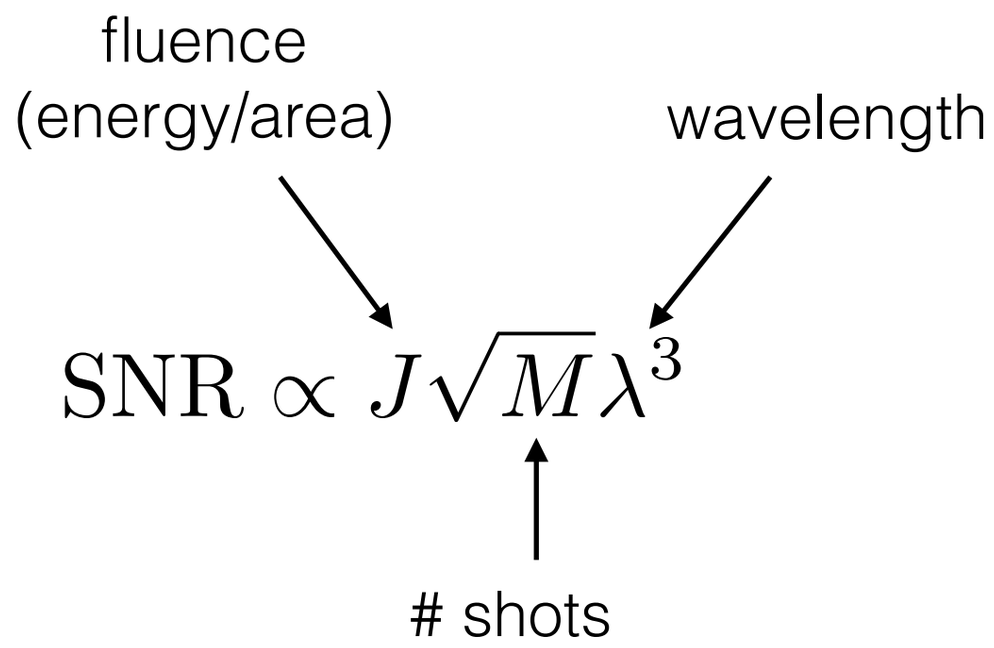

- This method could work with LCLS with 10^6 shots, *in absence of solvent scatter*
- With solvent, complete data at sub-nm resolution requires higher fluence
- We can begin working at low resolution, with partial data

Kirian, R. A., et al. (2011). Physical Review E, 84(1), 011921.

Signal may improve with continued XFEL developments

fluence (energy/area)

wavelength

$$\mathrm{SNR} \propto J\sqrt{M}\lambda^3$$

shots

Parameters at EuroXFEL potentially provide 5x15x15 ~ 1000-fold improved SNR over our previous calculations.

Proposal to generate 10 TW level femtosecond x-ray pulses from a baseline undulator in conventional SASE regime at the European XFEL

Svitozar Serkez ,[a,1] Vitali Kocharyan,[a] Evgeni Saldin,[a] Igor Zagorodnov,[a] Gianluca Geloni,[b]

[a]*Deutsches Elektronen-Synchrotron (DESY), Hamburg, Germany*

[b]*European XFEL GmbH, Hamburg, Germany*

Abstract

Output characteristics of the European XFEL have been previously studied assuming an operation point at 5 kA peak current. In this paper we explore the possibility to go well beyond such nominal peak current level. In order to illustrate the potential of the European XFEL accelerator complex we consider a bunch with 0.25 nC charge, compressed up to a peak current of 45 kA. An advantage of operating at such high peak current is the increase of the x-ray output peak power without any modification to the baseline design. Based on start-to-end simulations, we demonstrate that such high peak current, combined with undulator tapering, allows one to achieve up to a 100-fold increase in a peak power in the conventional SASE regime, compared to the nominal mode of operation. In particular, we find that 10 TW-power level, femtosecond x-ray pulses can be generated in the photon energy range between 3 keV and 5 keV, which is optimal for single biomolecule imaging. Our simulations are based on the exploitation of all the 21 cells foreseen for the SASE3 undulator beamline, and indicate that one can achieve diffraction to the desired resolution with 15 mJ (corresponding to about $3 \cdot 10^{13}$ photons) in pulses of about 3 fs, in the case of a 100 nm focus at the photon energy of 3.5 keV.

arXiv:1308.0448.

All aspects of the experiments are improving with time

We seek to measure **<u>weak signal</u>** for off-Bragg phasing, intensity correlations, and single-molecule diffraction

Time-resolved, direct imaging of proteins in solution and at room temperature would be monumental

We wish to have:

- Photon-discriminating detectors
- Increased dynamic range (~10^5)
- Higher data collection rates
- *Efficient, stable sample injectors* (@4.5 MHz)

Summary

- Serial crystallography is a powerful technique, and may be even more powerful if we fully exploit the continuum of diffraction intensities
- Solution scattering with an XFEL potentially reveals far more information than conventional wisdom holds. Developing intensity correlation measurements are a difficult but worthwhile endeavor.
- Source, detectors, injectors continue to develop at a rapid pace, making way for an increasingly rich variety of measurement strategies with XFELs